A Round Robin Test on Flash Thermography

Nick ROTHBART [1], Christiane MAIERHOFER [1], Matthias GOLDAMMER [2], Felix HOHLSTEIN [3], Joachim KOCH [4], Igor KRYUKOV [5], Guido MAHLER [6], Bernhard STOTTER [7], Günter WALLE [8], Beate OSWALD-TRANTA[9], Martin SENGEBUSCH[10]

[1] BAM Bundesanstalt für Materialforschung und -prüfung, Berlin, Germany
[2] Siemens AG Corporate Technology, München, Germany
[3] Block Materialprüfung GmbH, Berlin, Germany
[4] edevis GmbH, Stuttgart, Germany
[5] Universität Kassel, Kassel, Germany
[6] InfraTec GmbH Infrarotsensorik und Messtechnik,
[7] FH Oberösterreich, Wels, Austria
[8] Fraunhofer-Institut für Zerstörungsfreie Prüfverfahren IZFP, Saarbrücken, Germany
[9] University of Leoben, Leoben, Austria
[10] Deutsches Institut für Normung e. V.

Contact e-mail: christiane.maierhofer@bam.de

Abstract. A round robin test on flash thermography was organized within the scope of a standardization research project. This test gives information on reliability, comparability and efficiency of different testing situations. Data recorded on metal and CFRP test specimens with flat bottom holes (FBH) were analysed by evaluating the detectability and by calculating the signal-to-noise ratio (SNR) of the defect signatures as a function of defect parameters. For the investigation of the influence of material properties on the spatial resolution as well as on penetration depth, test specimens made of steel and copper with crossed notches and a notch ramp were constructed and investigated. Here, the minimum resolvable notch distance and the maximum detectable depth of the ramp were analysed.

1. Introduction

For testing structures of new lightweight constructions with thin cross sections, active thermography and especially flash thermography is very well suited as it has a high sensitivity for detecting defects situated close to the surface [1-3]. Flash thermography is fast, gives direct images, can be applied without any direct contact to the surface and thus reveals optimum conditions for the integration into production processes. Despite the great potential there are no application standards, reference samples or round robins on flash thermography available so far. These are necessary in order to unify measurement procedures or compare e.g. the influence of various measurement and material parameters. The only known round robin tests for active thermography were conducted in 1998 and 2000 using carbon fibre reinforced polymer (CFRP) specimens with impact damage [4, 5]. The aim of the trials of the former Eurotherm working group was to compare different excitation and evaluation techniques of active thermography by assessing the signal-to-noise ratio (SNR) of the detected flaws. Among other thermographic excitation methods,

also flash thermography was evaluated. While flash thermography reached a higher spatial resolution, only data evaluation using pulse phase thermography (PPT) [6] yielded to SNR values comparable to other excitation methods.

Thus, within the scope of a standardization project, a flash thermography round robin test that evaluates reliability, comparability and efficiency of the method for different testing situations was organized [7]. The results give information about the detectability of defects e.g. by their size, their depth, the evaluation method or by the materials used. Besides, the influence of equipment and parameters used by the participants on the results was analysed. However, the main purpose of the round robin test is not to compare the participants' results with respect to each other. Instead, the quantitative results as well as the feedback given by the participants will be presented in a DIN standardization committee in order to contribute to a new flash thermography standard for practical applications.

For the round robin test, sixteen test samples were made of steel, copper, aluminium and CFRP with unidirectional and quasi isotropic fibre orientation. Defects are simulated by flat bottom holes, crossed notches, notch ramps, delaminations made by thin PTFE layers between the CFRP layers and impact defects in CFRP of different energies. The measurements to be done were defined by detailed instructions that include measurements in reflection as well as in transmission configuration. In this contribution the round robin test and results concerning the detectability of flat bottom holes (FBH), the analysis of the SNR of selected FBH in phase images, the determination of spatial resolution at the crossed notches and the penetration depth at the notch ramp are presented. This project was performed together with DIN e. V. and was funded by the Federal Ministry for Economic Affairs and Energy within the research program INS Innovations by Norms and Standards.

2. Experimentals

Nine institutions from different backgrounds participated in the round robin test. These included universities, research institutes, industrial companies as well as small and medium enterprises. Together with the DIN e. V. as project manager, they are listed in the authorship.

2.1 Test Specimens

Three large metal test specimens with a size of 200 x 200 x 7.5 mm^3 and three small test specimens with a size of 100 x 100 x 4.5 mm^3 made of stainless steel (1.4301, X5CrNi18-10), aluminium (3.3206, AlMgSi0.5), and copper (CW004A) and with FBH of different sizes were constructed. For the large test specimens, the diameters of the holes were 8, 16 and 32 mm, and the remaining wall thicknesses (RWT) were varied between 2 and 6 mm. The small test specimens contained FBH with diameters of 1, 2 and 4 mm with RWT of 0.2 to 3.5 mm. For CFRP, only one test specimen was assembled containing FBH with diameters of 4, 8, 16 and 24 mm and with RWT from 0.5 to 3.5 mm. It has to be considered that the geometry of this test specimen was different from the other large test specimens. Two test specimens made of steel and copper were prepared with crossed notches with a notch width of 3 mm at one side and of 4 mm at the other side. The coverage of these crossed notches was 2 mm. Additionally, these specimens contained a notch ramp with a width of 3 mm and RWT from 2 to 5 mm. Sketches of the test specimens are visualised in figure 1. A blackening of the surfaces was performed using graphite spray for enhancing the emissivity. The same graphite spray was recommended to be used by all participants during the round robin test. The thermal parameters of all materials used are summarized in table 1.

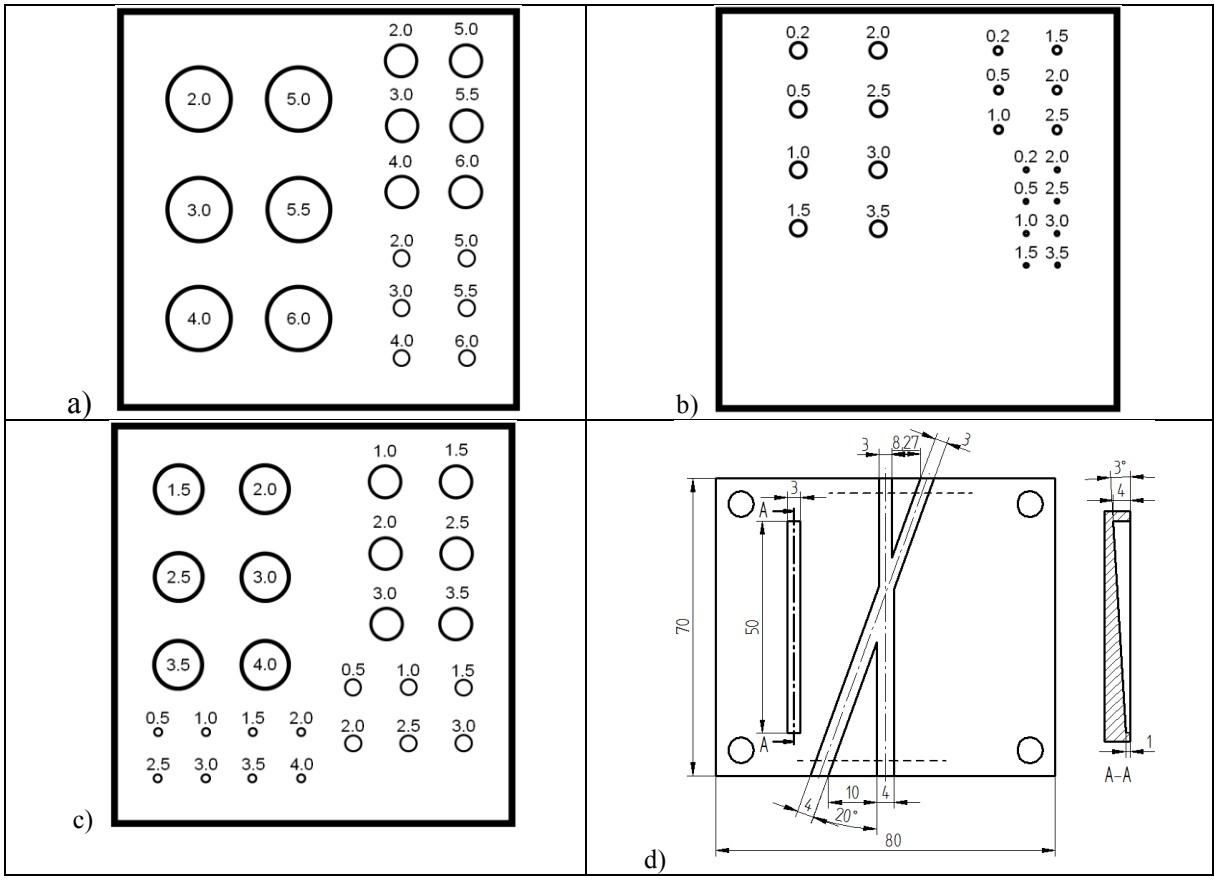

Fig. 1. Sketches of a) large metal test specimens with sizes of 200 x 200 x 7.5 mm^3 and FBH with diameters of 8, 16, and 32 mm, b) small metal test specimens with sizes of 100 x 100 x 4.5 mm^3 and FBH with diameters of 1, 2, and 4 mm, c) CFRP test specimen with sizes of 200 x 200 x 6 mm^3 and FBH with diameters of 4, 8, 16, and 24 mm and d) test specimens with crossed notches and notch ramps. The numbers are related to mm and in the FBH, these are related to the remaining wall thickness.

Table 1. Thermal material parameters of the test specimens of the round robin test

Material	**Diffusivity α in 10^{-5} m^2/s**	**Mass density ρ in kg/dm^3**	**Heat capacity c in J/(kg K)**	**Thermal conductivity λ in W/(m K)**
steel 1.4301 X5CrNi18-10	0.37 ± 0.02	7.9[a]	500[a]	14.6 ± 0.8
aluminium 3.3206 AlMgSi0.5	5.0 ± 0.2	2.7[b]	900[c]	121 ± 5
copper CW004A	9.8 ± 0.4	8.93[d]	386[d]	338 ± 14
CFRP with quasi-isotropic fibre alignment	0,025 ± 0.002[e]	1.5[f]	1200[g]	0.45 ± 0.04

[a] www.thyssenkrupp.at
[b] www.retsch.dk
[c] http://www.aluminiumdesign.net/why-aluminium/material-comparison/
[d] www.kupferinstitut.de
[e] perpendicular to fibre orientation
[f] www.swiss-composite.ch
[g] www.aviogate.com

2.2 Flash Thermography and Data Analysis

The minimum requirements concerning the specifications of the equipment and the measurement parameters to be used by each partner in the round robin test were given and had to be fulfilled. Thus, for thermal excitation, one to four flash lamps with flash durations from 1 to 11 ms were used. Total energies between 6 and 24 kJ were converted. With this energy, the measured temperature rise of a defined sensor plate was between 0.8 and 24 K. By considering the known heat capacity of this silver plate (0.242 J/K) and its surface size of 1 cm², this corresponds to an input energy density between 0.2 and 5.8 J/cm².

With the exception of one microbolometer infrared (IR) camera with 384 x 288 pixels, all IR cameras used contained indium antimonite (InSb) sensors with sizes of 320 x 256 to 640 x 512 pixels. All InSb cameras were sensitive in the mid wave infrared range (MWIR) between 1.5 to 5.7 µm and less. For the investigations at the test specimens, frame rates between 50 Hz (recommended frame rate for steel) and 353 Hz (300 Hz was recommended for copper and aluminium) were selected. The integration times were set between 720 and 2500 µs resulting in temperature resolutions (noise equivalent temperature difference NETD) between 40 and 18 mK. The distances of the flash lamps to the sample and of the IR camera to the sample were varying between 24 and 80 cm and 33 and 81 cm, respectively. The angles of the flash lamps to the normal of the sample surfaces were set between 0 and 45°.

Data analysis was performed by first subtracting one of the thermograms recorded before the flash from the whole thermal sequence. Afterwards, a thermogram from the recorded cooling down sequences providing an optimum temperature contrast of the defects was selected. PPT was applied to the data recorded after the flash and phase images providing again an optimum phase contrast of the defects were chosen. From these images, the detectability of all visible FBH in the thermograms and phase images was documented. The SNR of all defects in the selected thermograms and phase images of the large steel test specimen and of the FBH with a diameter of 16 mm and a RWT of 3 mm of the other materials were determined. Here, the signal intensity is equal to the maximum temperature or phase difference related to the sound material:

$$SNR_T = \frac{\Delta T}{\sigma_T}, \quad SNR_\varphi = \frac{\Delta \varphi}{\sigma_\varphi} \qquad \text{(eq. 1)}$$

The temperature and phase differences, ΔT and Δφ, respectively, were determined from the difference of the maximum of the signal of each FBH and the background close to the hole in respective line scans. In case of uncalibrated IR cameras, intensity values were used instead of temperature values. The noise σ was calculated from the standard deviation of the temperature or phase values inside an undisturbed area of the test specimen.

For the determination of the spatial resolution between the crossed notches with widths of 3 and 4 mm, first of all the phase images with the highest phase contrast should be selected. These were between 0.2 and 0.4 Hz for the steel test specimen and between 2.6 and 5 Hz for the copper test specimen. In these phase images, on each side at a distance of 10 mm to the edge the difference of the temperature above the notch and above the gap was calculated and was related to the noise. Thus two SNR values of the notch contrast were calculated. These positions correspond to an inner distance of 4.7 mm for the 3 mm wide notches and of 6.4 mm for the 4 mm wide notches. Additionally, for each pair of notches a minimum inner distance was calculated, where the notch contrast SNR was still > 1. The notch ramps were used for the determination of the penetration depth for detecting a 3 mm wide notch. From the sequences, phase images were calculated and those with the highest penetration depth were selected. The largest detectable RWT of the notch ramp was set at a position, where the ramp still could be detected with an SNR > 1.

3. Results

3.1 Detectability of Defects

The detectability of the defects in each test specimen is displayed in figure 2. Here it is shown how often each FBH could be detected by the nine participants. In the steel test specimen (figure 2.a) the holes with a diameter of 32 mm and RWT from 2 to 4 mm could be detected by all participants, while the hole with a diameter of 8 mm and a RWT of 6 mm could be detected only by three participants. The smaller number of detections of deeper holes can be explained by the limited penetration depth within the model of thermal waves. Holes with smaller diameters are detected less often (for similar RWT), as the contrast is reduced by lateral heat diffusion processes. For the larger aluminium test specimen (see figure 2.c), the data are more or less similar to the steel test specimen. For the larger copper test specimen (see figure 2.e), all deeper FBH could be detected less often than for the other materials. For the small test specimens, there is a larger difference between the detectability of the FBH in steel and in aluminium, where less FBH could be detected in aluminium. In CFRP, a bit less FBH with a diameter of 8 mm and similar RWT could be detected than in copper.

The number of all detected FBH in each test specimen (and thus for each material) and for each participant is visualized in the diagrams in figure 3. First of all, from these diagrams it is obvious that the number of detected holes is very low for participant D, who used the microbolometer IR-camera. For the other participants, the number of detected holes in steel and CFRP is similar, while the participants are divided into two groups concerning the detection of FBH in copper. While this number was higher for participants A, B, C and E, it was lower for participants F, G, H and I. Partly, this could be explained by the used frame rates as well as by the procedures, which were used for calculating the phase images.

3.2 Signal-to-Noise Ratio

For each material and each participant, the SNR values of the FBH with a diameter of D = 16 mm and a RWT of d = 3 mm was calculated from the phase images according to eq. 1. The results are shown in the diagram in figure 4.a together with the mean values for each material. This diagram clearly shows that for steel and aluminium, a similar mean SNR value was obtained while the lowest mean SNR value was obtained for copper. It is obvious that there appeared a large scattering between the different participants. Therefore, the SNR value of the same FBH was averaged over all materials for each participant, see figure 4.b. With the exception of participant D, again the same two groups of participants could be separated.

3.3 Spatial Resolution and Penetration Depth

The results concerning the determination of the contrast values of the 3 mm and 4 mm wide notches at an inner distance of the two notches of 4.7 mm and 6.4 mm, respectively, are shown in the diagram in figure 5.a. Here, the SNR in steel is significantly higher than in copper. The minmum resolveable distances of the two notch pairs in copper and steel are depicted in figure 5.b. A significantly higher resolution was obtained for steel, where the 3 mm wide notches could be resoved down to a mean distance of 1.2 mm. Figure 6.a and b show the maximum obtained penetration depths in the two materials. Although less particpiants could detect the notch ramps in copper, the maximim achieved penetration depth was more or less similar in both materials.

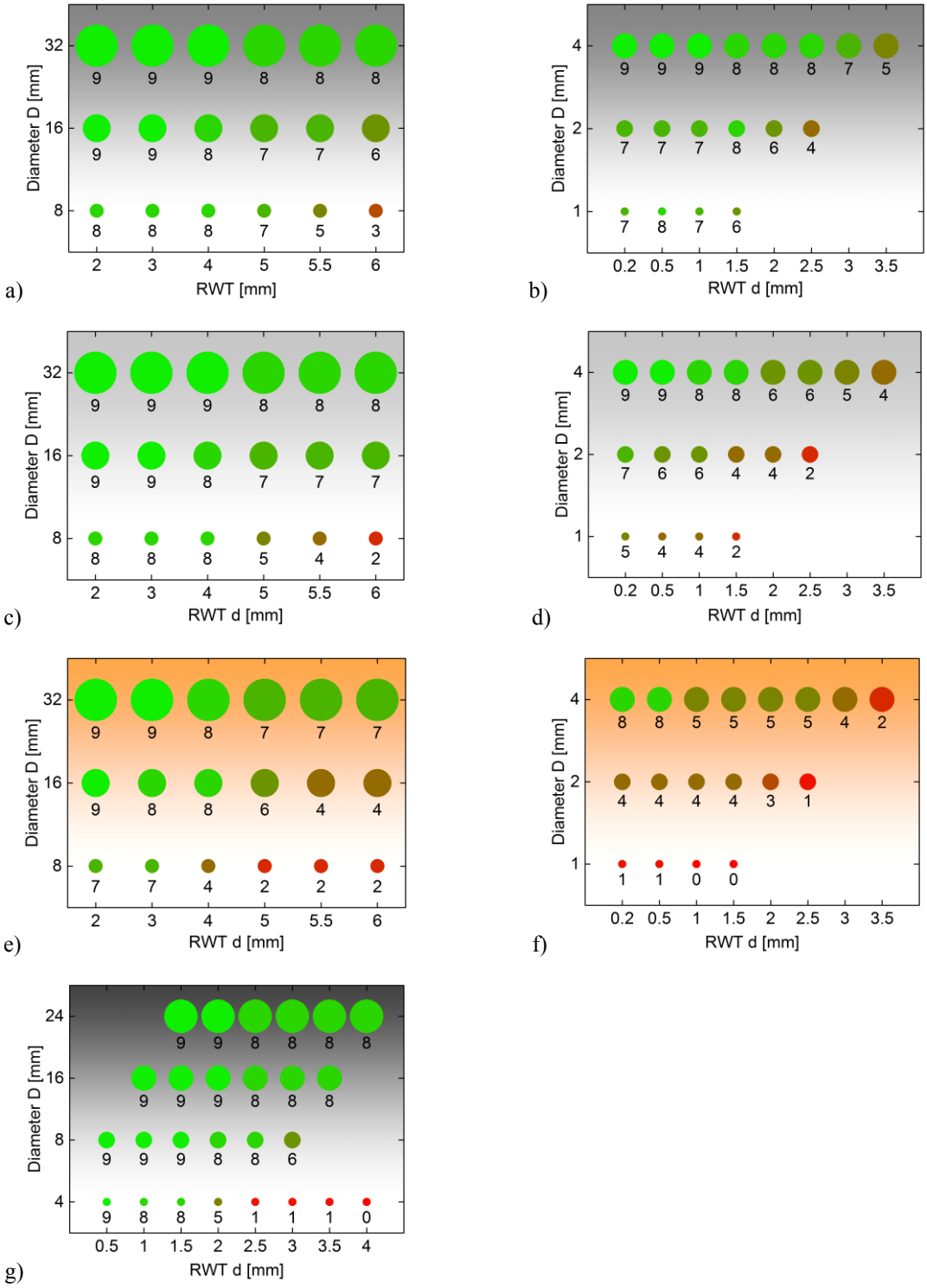

Fig. 2. Detectability of flat bottom holes in a, b) steel, c, d) aluminium, e, f) copper and g) CFRP as a function of hole diameter D and remaining wall thickness d for all nine participants, thus the maximum number of detections for each FBH was 9.

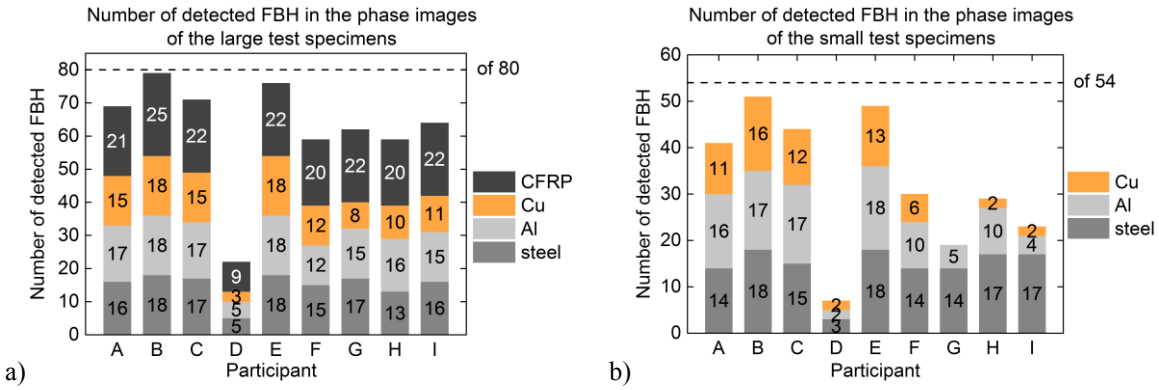

Fig. 3. Number of detected flat bottom holes for each participant and each material in a) the large test specimens and b) the small test specimens.

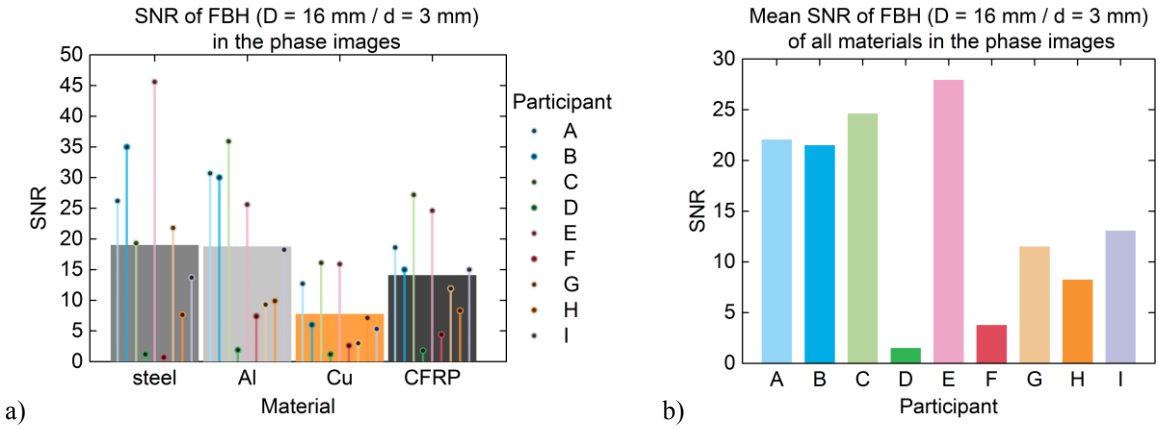

Fig. 4. a) Mean SNR and SNR of each participant of the FBH with D = 16 mm and a RWT of d = 3 mm for all materials. b) SNR of each participant of the FBH with D = 16 mm and d = 3 mm averaged over all materials. The SNR values are related to the phase images.

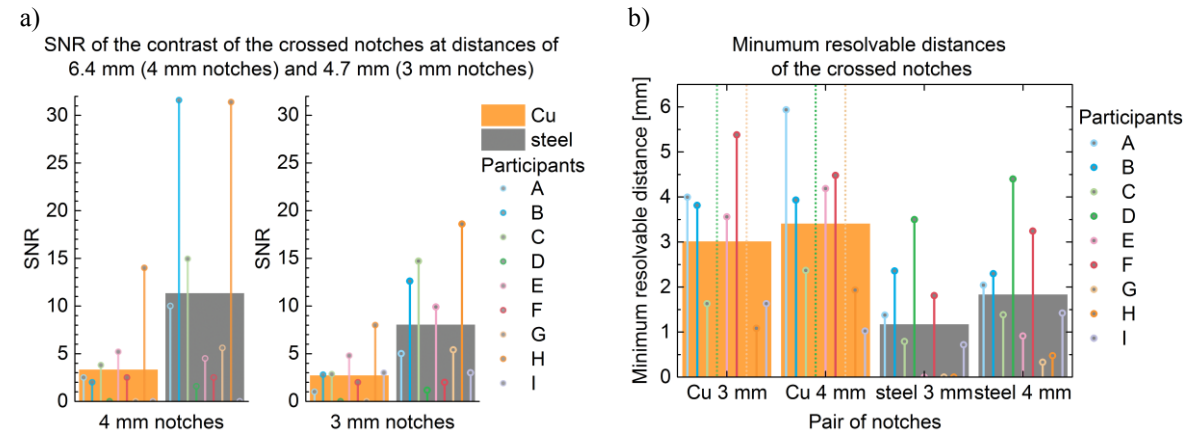

Fig. 5. a) Mean SNR and SNR of each participant of the contrast value of the 3 mm and 4 mm wide notches at an inner distance of the two notches of 4.7 mm and 6.4 mm, respectively. b) Mean value and value of each participant of the minimum resolvable distance of the 3 mm and 4 mm wide notches. Both diagrams show the values obtained in copper and steel in the phase images.

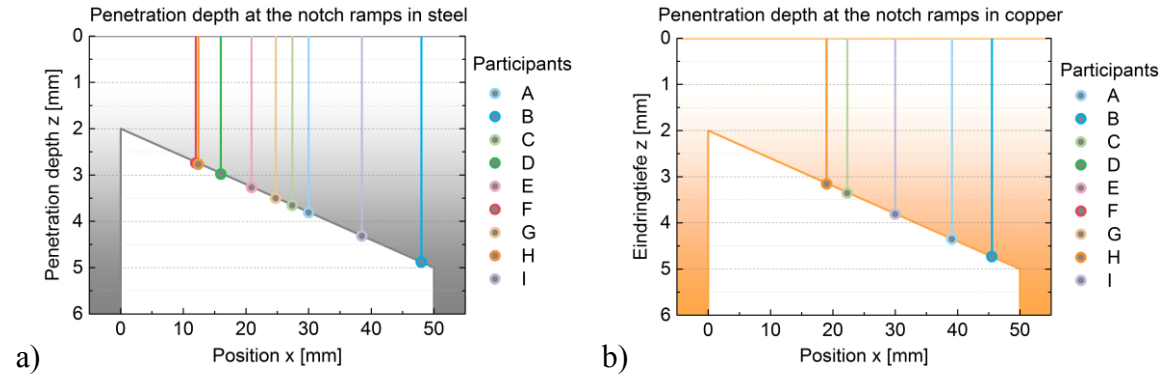

Fig. 6. Maximum detected RWT thicknesses of the 3 mm wide notch ramps in a) steel and b) copper, depicted for each participant.

4. Conclusion

From the results of the investigations at the FBH as well as at the crossed notches, it can be concluded that the detectability of the holes and the spatial resolution is strongly influenced by the type of the material, i. e. the most holes could be detected in steel and the fewest in copper, and the highest spatial resolution was obtained in steel. Although by all participants a similar number of holes was detected in steel and CFRP, stronger deviations were observed for aluminium and copper. The maximum penetration depth obtained in both materials was similar, although some participants were not able to detect the notch ramp in copper.

Acknowledgements

The project was funded within the program Innovations with Norms and Standards (INS 1255) by the German Federal Ministry of Economics and Energy. Within DIN e. V., the Standards Committee Materials Testing (NMP) was responsible for the project.

References

[1] Shepard, S.M., Advances in pulsed thermography. Proc. SPIE 4360, Thermosense XXIII, 511 (March 23, 2001); doi:10.1117/12.421032

[2] Maierhofer, C., Röllig, M., Ehrig, K., Meinel, D., Céspedes-Gonzales, G.; Validation of flash thermography using computed tomography for characterizing inhomogeneities and defects in CFRP structures. Composites Part B: Engineering, Volume 64, August 2014, Pages 175-186

[3] Vavilov, V.P., Burleigh, D.D. Review of pulsed thermal NDT: Physical principles, theory and data processing. NDT & E International 73 (2015) 28-52

[4] Vavilov, V. P., Almond, D. P., Busse G., Grinzato E., Krapez J-C.,Maldague X., Marinetti, S., Peng, W., Shirayev, V., Wu, D.: Infrared thermographic detection and characterisation of impact damage in carbon fiber composites: results of the round robin test. QIRT 1998, Lodz, Poland

[5] Almond, D. P., Ball, R. J., Dillenz, A., Busse, G., Krapez, J.-C., Galmiche, F., Maldague X.: Round Robin comparison II of the capabilities of various thermographic techniques in the detection of defects in carbon fibre composites. QIRT 2000, http://qirt.gel.ulaval.ca/archives/qirt2000/papers/065.pdf

[6] Maldague, X., Galmiche, F., Ziadi, A.; Advances in pulsed phase thermography. Infrared Physics & Technology 43 (2002) 175–181.

[7] Rothbart, N., Maierhofer, C., Goldammer, M., Hohlstein, F., Koch, J., Kryukov, I., Mahler, G., Stotter, B., Walle, G., Oswald-Tranta, B., Sengebusch, M. A round robin test of flash thermography of CFRP and metal structures. In: Proceedings of 7th International Symposium on NDT in Aerospace 2015, Mo.4.A.5